Mind blanking is a distinct mental state linked to a recurrent brain profile of globally positive connectivity during ongoing mentation

Mortaheb, Sepehr; Van Calster, Laurens; Raimondo, Federico; Klados, Manousos A.; Boulakis, Paradeisios Alexandros; Georgoula, Kleio; Majerus, Steve; Van De Ville, Dimitri; Demertzi, Athena

How to cite

MORTAHEB, Sepehr et al. Mind blanking is a distinct mental state linked to a recurrent brain profile of globally positive connectivity during ongoing mentation. In: Proceedings of the National Academy of Sciences of the United States of America, 2022, vol. 119, n° 41, p. e2200511119. doi: 10.1073/pnas.2200511119

This publication URL: https://archive-ouverte.unige.ch/unige:175639

Publication DOI: 10.1073/pnas.2200511119

PNAS RESEARCH ARTICLE | PSYCHOLOGICAL AND COGNITIVE SCIENCES

Mind blanking is a distinct mental state linked to a recurrent brain profile of globally positive connectivity during ongoing mentation

Sepehr Mortaheb[a,b], Laurens Van Calster[a,b], Federico Raimondo[c,d], Manousos A. Klados[e], Paradeisios Alexandros Boulakis[a,b], Kleio Georgoula[a], Steve Majerus[a,b,f], Dimitri Van De Ville[g,h,1], and Athena Demertzi[a,b,f,1,2]

Edited by Jonathan Schooler, University of California at Santa Barbara, Santa Barbara, CA; received January 11, 2022; accepted August 30, 2022 by Editorial Board member Michael S. Gazzaniga

Mind blanking (MB) is a waking state during which we do not report any mental content. The phenomenology of MB challenges the view of a constantly thinking mind. Here, we comprehensively characterize the MB's neurobehavioral profile with the aim to delineate its role during ongoing mentation. Using functional MRI experience sampling, we show that the reportability of MB is less frequent, faster, and with lower transitional dynamics than other mental states, pointing to its role as a transient mental relay. Regarding its neural underpinnings, we observed higher global signal amplitude during MB reports, indicating a distinct physiological state. Using the time-varying functional connectome, we show that MB reports can be classified with high accuracy, suggesting that MB has a unique neural composition. Indeed, a pattern of global positive-phase coherence shows the highest similarity to the connectivity patterns associated with MB reports. We interpret this pattern's rigid signal architecture as hindering content reportability due to the brain's inability to differentiate signals in an informative way. Collectively, we show that MB has a unique neurobehavioral profile, indicating that nonreportable mental events can happen during wakefulness. Our results add to the characterization of spontaneous mentation and pave the way for more mechanistic investigations of MB's phenomenology.

mind blanking | experience sampling | resting state | mental content | functional connectivity

Significance

The human mind is generally assumed to be constantly thinking. The phenomenology of mind blanking (MB) challenges this stance because it appears that we can be deprived of mental contents, or at least consciously preceiving them. We here show that, during spontaneous thinking, MB is a mental state that happens by default, it has a unique behavioral profile, and it is linked to a rigid neural architecture that does not permit us to report thoughts. This work corroborates that nonreportable mental events can happen during wakefulness, which challenges the view that the mind is constantly occupied by reportable thoughts.

During spontaneous experience our mentation is ongoing, dynamic, and rich in content (1), taking the form of mental states. Mental states are transient cognitive or emotional occurrences that are described in terms of content (what the state is "about") and the relation we bear to this content (e.g., imagining, remembering, fearing) (2). In that sense, thoughts are sequences of mental states (2). Thoughts can be self-related or can refer to others, they can be about the future or past, and they can happen in task-free conditions (3) or when off-task (4, 5). We can also have perceptual content during which external stimuli are perceived through our senses and internal stimuli are perceived via our interoceptive system (3). Contemporary views of ongoing thought see spontaneous experience as an interplay between idiosyncratic processes (e.g., self-generated thoughts) and environmental demands (e.g., task difficulty). For example, off-task thoughts and daydreaming can be observed more frequently when environmental demands are less pronounced (5). Altogether, these mental experiences suggest that our mind is generally constantly thinking.

Interestingly, ongoing experience can also show moments when we cannot report any mental content, often accompanied by a post hoc realization that our mind "went away" (6) or got blanked (7). This particular phenomenon is often referred to as mind blanking (MB). MB has been defined as "reports of reduced awareness and a temporary absence of thought (empty mind) or lack of memory for immediately past thoughts [that] can be considered as the phenomenological dimension of a distinct kind of attentional lapse" (8). This definition implies that MB can have various mechanistic causes, such as lack of content meta-awareness, failure in memory retrieval, or lapses in attention. Regardless of the mechanistic counterpart, MB's phenomenology challenges the view of the mind as relating primarily to thoughts. Given this observation, what is the relation between MB and other mental states and what are the specific neural configurational processes that support this phenomenology?

To date, behavioral and neuroimaging studies have shown that MB can be reported with a low frequency compared to other mental states, it can occur either during resting state (3) or during a cognitive task (9), and it can be accompanied by particular neural activity. Behaviorally, it has been shown that, during focused tasks, MB was reported on average 14.5% of the times whenever subjects evaluated their mental state

Author contributions: S. Mortaheb, L.V.C., S. Majerus, and A.D. designed research; S. Mortaheb, L.V.C., P.A.B., K.G., and A.D. performed research; S. Mortaheb, F.R., M.A.K., D.V.D.V., and A.D. contributed new reagents/analytic tools; S. Mortaheb analyzed data; and S. Mortaheb and A.D. wrote the paper.

The authors declare no competing interest.

This article is a PNAS Direct Submission. J.W.S. is a guest editor invited by the Editorial Board.

[1]D.V.D.V. and A.D. contributed equally to this work.

[2]To whom correspondence may be addressed. Email: a.demertzi@uliege.be.

This article contains supporting information online at http://www.pnas.org/lookup/suppl/doi:10.1073/pnas.2200511119/-/DCSupplemental.

Published October 4, 2022.

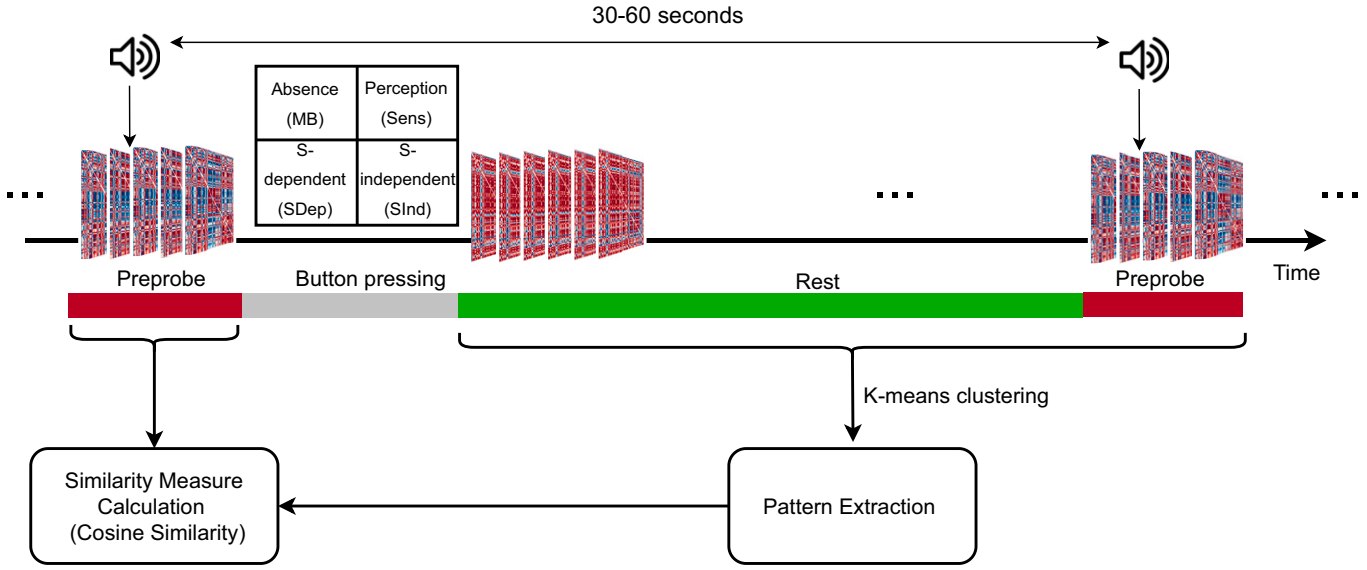

Fig. 1. Data acquisition and analysis paradigm. While at rest, participants were randomly interrupted by an auditory probe to report their immediate mental state choosing between absence (MB), Sens, SDep, and SInd. In order to estimate which brain configuration corresponded to a reported mental state, connectivity matrices were estimated via phase-based coherence for each fMRI volume. The matrices were then organized in distinct patterns via *k*-means clustering, and the similarity between these patterns and the matrices relating to the reported mental states of the preprobe period was calculated. The pattern with the highest similarity to the preprobe matrices was assigned to that reported mental state.

upon request (6) and 18% of the time when participants reported MB by self-catching (10). During resting state, this number was reported to be about 6% (3). Neuroimaging data showed that when participants were instructed to "think of nothing" as compared to "let your mind wander," there was lower functional MRI (fMRI) functional connectivity between the default mode network and frontal, visual, and salience networks (11). MB has also been associated with deactivation of Broca's area and parts of the hippocampus, as well as with activation of the anterior cingulate cortex, which was interpreted as evidence for reduced inner speech (7). Decreased functional connectivity in the posterior regions of the default mode network and increased connectivity in the dorsal attentional network was also found in an experienced meditator practicing content-minimized awareness, which can be considered a phenomenological proxy to sustained MB (12).

Collectively, these studies indicate that the investigation of MB is rising over the years. Yet, we observe that its neurobehavioral characterization remains inconclusive for several reasons. First, MB has been studied after deliberately inducing it or in highly trained individuals; therefore, its spontaneous occurrences are not generalizable. Second, in some cases MB has been studied in isolation from other mental states; therefore, its interstate dynamics are lacking. Third, current MB's neural correlates concern a limited number of brain regions, leaving the whole-brain functional connectome uncharted. Here, we aimed at addressing these issues by delineating the neurobehavioral profile of MB in a comprehensive way. For this purpose, we used fMRI-based experience sampling in typical individuals (3) in order to account for the behavioral quantification of spontaneous (noninduced) MB occurrences, determine MB's intermental state dynamics, and estimate MB's functional fine-grained connectome at the whole-brain level.

Results

We used previously acquired data (3) collected from 36 healthy participants (27 women, 9 men, mean age: 23 y ± 2.9) within a 3-T MRI scanner while they were at rest with eyes open. Experience-sampling concerned randomly presented sounds ($n = 50$) that prompted the participants to evaluate and choose by button press the mental states in which they were engaged prior the probe. Possible mental states were absence (i.e., MB), perception of sensory stimuli (Sens), stimulus-dependent thoughts (SDep), and stimulus-independent thoughts (SInd) (Fig. 1).

Behavioral Analysis. Considering the occurrence rate over time, MB was reported significantly fewer times than the other mental states (median = 2.5, IQR = 3, min = 0, max = 9; Fig. 2*A*). With respect to reaction times, there was a main effect of mental state ($\chi^2[3] = 66.63$, $P < 0.001$; generalized linear mixed model analysis; Fig. 2*B*), with MB being reported faster than SDep ($z = 3.81$, $P = 0.0008$) and SInd ($z = 3.37$, $P = 0.0042$) but with no significant differences from Sens ($z = -0.73$, $P = 0.89$; post hoc Tukey test). The evaluation of the dynamic transitions between different mental states showed exceptionally low but equal probabilities (0.06) for reporting MB when departing from a content-oriented state (Fig. 2*C*). Also, the probability of rereporting MB was particularly low (0.04). Finally, the hypothesis of a uniform distribution of reports across the session could not be rejected for MB ($\chi^2[9] = 12.31$, $P = 0.20$, $\varphi = 0.35$), SDep ($\chi^2[9] = 5.25$, $P = 0.81$, $\varphi = 0.10$), or SInd ($\chi^2[9] = 4.22$, $P = 0.90$, $\varphi = 0.07$). Sens reports, though, were not uniformly distributed over time ($\chi^2[9] = 18.15$, $P = 0.03$, $\varphi = 0.23$; *SI Appendix*, Fig. S1).

fMRI Analysis.

MB is associated with a distinct physiological state. To estimate the MB's functional connectome, we first sought to delineate the contribution of the global signal (GS). This was because the GS has been previously shown to contain neural sources (13–15) and thus can be of functional significance. The spatially averaged time series were extracted from the regions of interest (ROIs), and their amplitude was estimated for five volumes (10.2 s) per probe, that is, two volumes preceding the probe and three after it (Fig. 1) to account for the blood oxygen level–dependent (BOLD) hemodynamic response (see *Methods*), and their mean absolute value was calculated. By using this 10-s analysis window, we found a significant effect of mental state on the GS amplitude

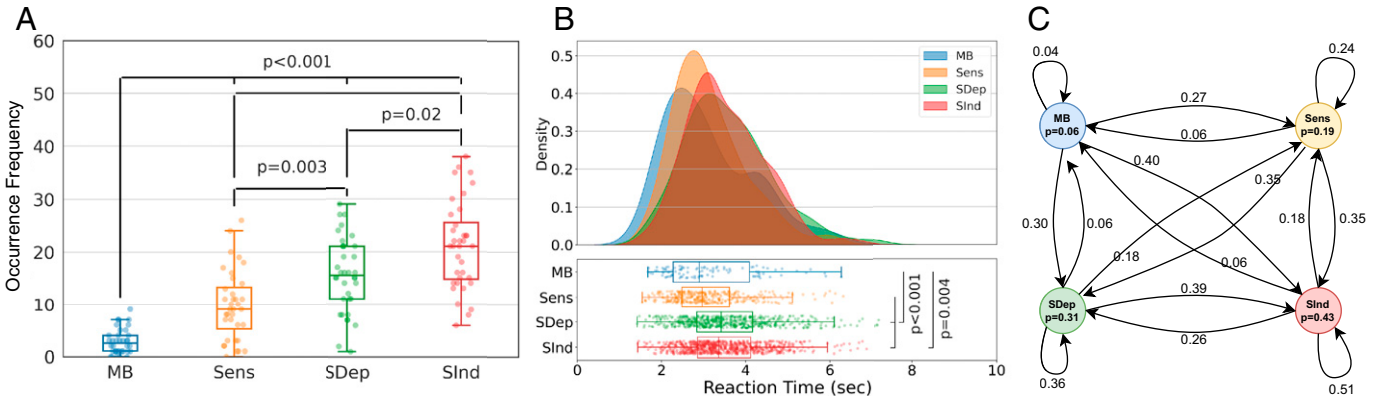

Fig. 2. Mind Blanking (MB) is characterized by a distinct behavioral profile. (*A*) MB shows significantly low reportability by comparison to the other mental states, replicating past findings (FDR $P < 0.05$). (*B*) MB is reported significantly faster than SDep and SInd mental states, possibly reflecting shorter cognitive evaluation due to the "absent content" as opposed to thought-related reports. (*C*) The Markov model shows that the probability of reporting an MB state after exploring other mental states is low but equal (6%), suggesting that MB might serve as a transient mental relay during spontaneous mentation. Sens, sensory perception of stimuli; SDep, stimulus-dependent thoughts; SInd, stimulus-indepedent thoughts.

($\chi^2[3] = 12.474$, $P = 0.006$; generalized linear mixed model), with higher amplitude relating to the volumes surrounding MB reports as compared to those linked to SDep ($z = 3.3$, $P = 0.005$) and SInd reports ($z = 2.55$, $P = 0.05$; post hoc Tukey test; Fig. 3). Similar results were obtained when the analysis window lagged between zero frames (i.e., five scans preprobe) up to three volumes (i.e., two preprobe and three postprobe scans; *SI Appendix*, Fig. S2). As the GS contributes deferentially to the reportability of mental states, we decided to include it in the connectivity analyses. For comprehensive purposes, all analyses were performed without the GS as well. To investigate the potential effect of the level of arousal on MB reportability, we also calculated the correlation between the GS amplitude and the reaction times of all MB reports. No significant correlation was found (Spearman's $\rho = 0.03$, $P = 0.76$; *SI Appendix*, Fig. S2).

MB is accurately classified by means of phase-based coherence. To check whether MB is of distinct neural profile, we first tested whether it can be classified among other mental states by using the functional connectome. Using the Hilbert transform, we estimated framewise phase-based coherence matrices for the above-mentioned period of five volumes (lag = 3). Considering these connectivity matrices as feature vectors (five vectors per probe), a support vector machine (SVM) classifier with fivefold cross-validation and 10 repeats classified MB reports from all mental states with an average precision of 1, average recall of 0.81, and average balanced accuracy of 0.90. In addition, a one-versus-one strategy to classify MB from the other reports separately led to high classification performance (Table 1). To compare the results with the empirical chance level, a dummy classifier was further used to separate MB-labeled matrices from the matrices corresponding to the other mental states. This dummy classifier generated random predictions by respecting the training set class distribution (Table 1). This classification strategy also showed comparable performance for other analysis window lag values (*SI Appendix*, Tables S1–S4). Collectively, by comparing all the performance metrics of the MB classification by using an SVM and the dummy classifier, we found that the SVM successfully separated the functional connectomes of MB reports from those belonging to the other mental states.

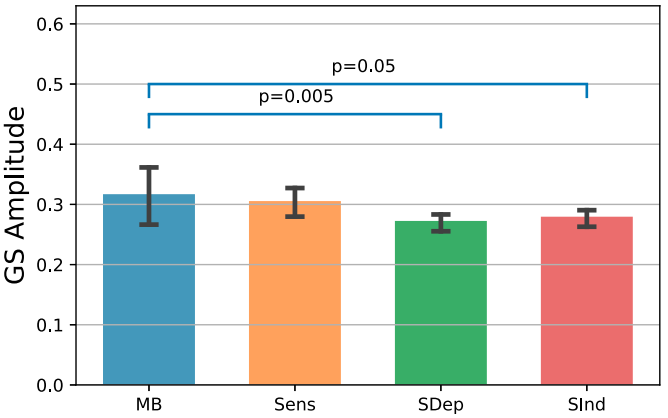

Fig. 3. Volumes labeled as Mind Blanking (MB) are characterized by high global signal (GS) amplitude. The average absolute value of the GS shows that the GS amplitude is significantly higher for volumes reportes as MB compared to the GS amplitude observed in volumes reporting content-oriented states, pointing to a distinct physiological substrate supporting MB reportability. Bars show the mean absolute value, and error bars show 95% CIs. Sens, sensory perception of stimuli; SDep, stimulus-dependent thoughts; SInd, stimulus-indepedent thoughts.

Functional connectivity organizes into distinct recurrent patterns. Under the hypothesis that the MB's neural signature is contained in connectivity dynamics, we investigated how the framewise functional connectome organizes into distinct connectivity patterns. By concatenating all the estimated connectivity matrices across subjects and by applying *k*-means clustering, we determined four main functional brain patterns that appeared recurrently across the resting state periods, replicating previous results (16) despite different acquisition parameters and parcellation schemes. The patterns were characterized by distinct signal configurations: a pattern of complex interareal interactions, containing positive and negative phase coherence values between long-range and short-range regions (pattern 1), a pattern showing anticorrelations primarily between the visual network and the other networks (pattern 2), a pattern with overall positive interareal phase coherence (pattern 3), and a pattern of overall low interareal coherence (pattern 4; Fig. 4*A*). In terms of occurrences, pattern 4 appeared at a significantly higher rate than pattern 1 ($t[35] = 7.131$, $P < 0.001$, Cohen's $d = 1.18$), pattern 2 ($t[35] = 7.495$, $P < 0.001$, Cohen's $d = 1.25$), and pattern 3 ($t[35] = 5.857$, $P < 0.001$, Cohen's $d = 0.98$, P values false discovery rate (FDR) corrected at $\alpha = 0.05$; Fig. 4*A*). Importantly, these patterns also emerged when we used different cluster sizes (ranging from 3 to 7) and different analysis window lags (ranging from zero up to three frames; *SI Appendix*, Figs. S3–S6).

Neurobehavioral Coupling. To determine which brain pattern was the closest to the MB reports, we used the cosine distance

Table 1. Performance of SVM classifier when predicting MB reports based on phase coherence matrices (lag = 3)

	Balanced accuracy	Recall	Precision
MB vs. Sens	0.97, CI = (0.87, 1)	0.95, CI = (0.75, 1)	0.99, CI = (0.98, 1)
MB vs. SDep	0.96, CI = (0.84, 1)	0.92, CI = (0.69, 1)	1, CI = (1, 1)
MB vs. SInd	0.94, CI = (0.81, 1)	0.88, CI = (0.61, 1)	1, CI = (1, 1)
MB vs. others	0.90, CI = (0.77, 1)	0.81, CI = (0.54, 1)	1, CI = (1, 1)
MB vs. others (dummy)	0.50, CI = (0.43, 0.57)	0.05, CI = (–0.07, 0.18)	0.06, CI = (–0.10, 0.22)

Recall is a parameter in the range of 0–1, which reflects the classifier's ability to identify positive samples correctly. Precision is a parameter between 0 and 1, which defines the ability of the classifier to not label as positive a sample that is negative.

as the similarity measure between five connectivity matrices of each analysis window and the four resting brain patterns (Fig. 1). Using a generalized linear mixed model fit to the distance measures of each brain pattern separately, we found a significant effect of mental state for distance values to pattern 3 ($\chi^2[3] = 19.088$, $P = 0.0002$). Pattern 3 further showed higher similarity to MB compared to the reports of Sens (estimate = 0.114, low CI = 0.027, high CI = 0.202, $P = 0.004$), SDep thoughts (estimate = 0.137, low CI = 0.053, high CI = 0.221, $P = 0.0002$), and SInd thoughts (estimate = 0.132, low CI = 0.050, high CI = 0.213, $P = 0.0002$; post hoc Tukey tests; Fig. 4*B*). These results were also replicated with different analysis window lags (*SI Appendix*, Figs. S16–S19).

For comprehensive purposes, we performed a supplementary analysis of the neurobehavioral coupling by omitting the GS through subtraction or regression. Global signal subtraction (GSS) refers to withdrawing the GS from the ROI preprocessed time series, while global signal regression (GSR) concerns removing the GS from the preprocessed ROI time series via linear regression. After GSS and GSR were applied, all brain patterns were reproduced except for pattern 3 (*SI Appendix*, Fig. S15*A*), whose architecture shifted toward negative coherence values. The same observation was noticed on the clustering results with different cluster sizes (*SI Appendix*, Figs. S7–S14). The overall effect of GSS and GSR on the connectivity patterns was the shift of connectivity value distributions toward negative values thus enhancing anticorrelations (17–19), also previously reported (20) (*SI Appendix*, Fig. S15*B*) (17–19). In addition, interpattern correlation analysis showed that pattern 3 had the lowest similarity to itself after GSS and GSR ($\rho = 0.59$; *SI Appendix*, Fig. S15*C*). Considering a $P < 0.05/4 = 0.0125$ threshold to correct for multiple tests, no significant effect of mental states on the similarity measures were found for any pattern, neither for GSS (pattern 1, $P = 0.931$; pattern 2, $P = 0.116$; pattern 3, $P = 0.294$; pattern 4, $P = 0.573$), nor for GSR (pattern 1, $P = 0.109$; pattern 2, $P = 0.022$; pattern 3, $P = 0.276$; pattern 4, $P = 0.093$);

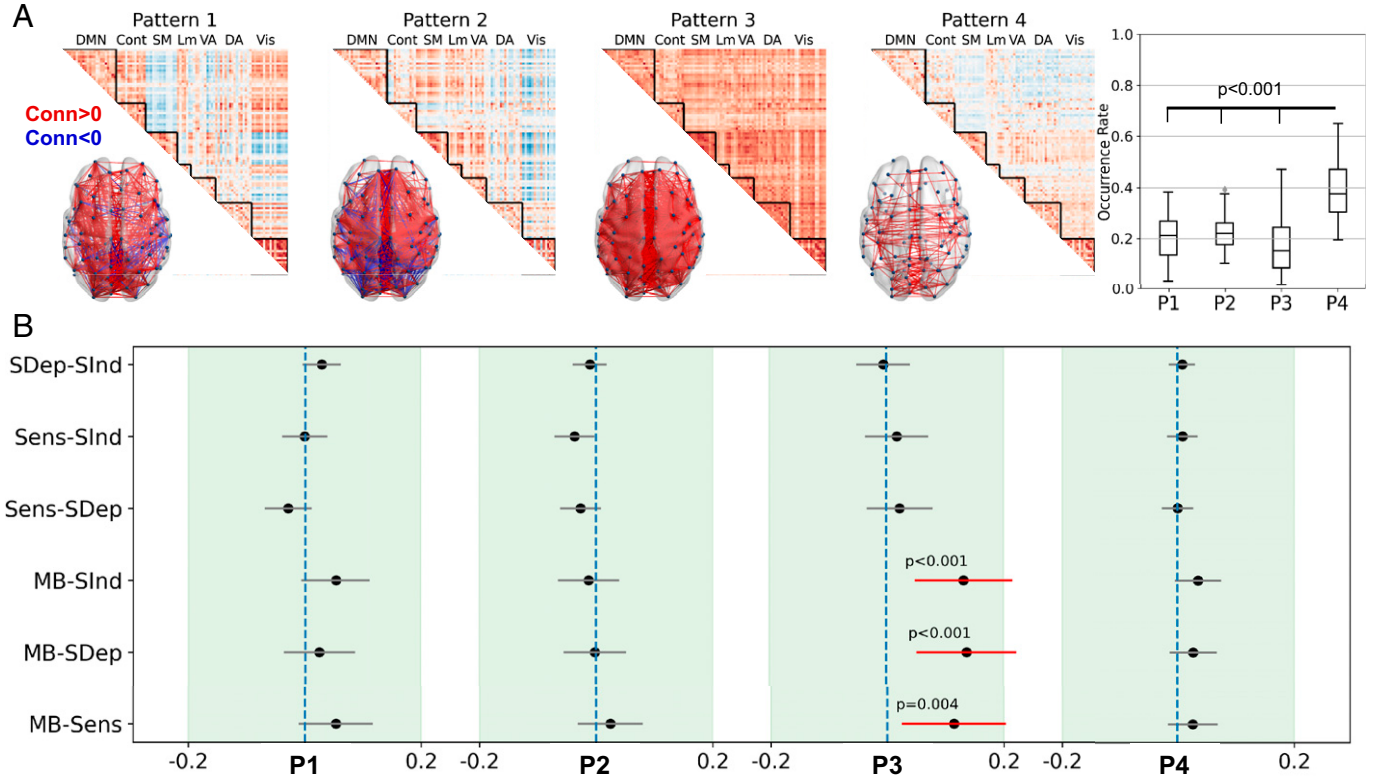

Fig. 4. MB is associated with an overall positive interregional brain connectivity pattern. (*A*) Brain functional organization during rest can be summarized into four main connectivity patterns of complex cortical interactions (pattern 1 [P1]), visual network anticorrelations (pattern 2 [P2]), globally positive coherence (pattern 3 [P3]), and low interareal connectivity (pattern 4 [P4]). There were similar occurrences rates across patterns, except for P4, which potentially reflects the underlying anatomy and therefore acts as a foundation upon which the others can occur. (*B*) The globally positive phase coherence P3 shows the highest similarity (positive contrast value of cosine similarity) to the connectivity matrices related to the MB reports compared to the other mental states. Black dots show the difference between similarity measures to the related connectivity pattern for each pair of mental states; error bars indicate 95% CIs; vertical blue lines indicate the zero differences. Conn, connectivity (phase-based coherence); DMN, default mode network; Cont, executive control network; DA, dorsal attentional network; VA, ventral attentional network; Lm, limbic network; Vis, visual network; SM, somatomotor network.

SI Appendix, Figs. S20 and S24). These results suggest that the GS carries partially independent neural information and contributes to the cerebral profile of MB reportability.

Discussion

We used experience sampling paired with fMRI to determine the neurobehavioral profile of MB in typical individuals in order to delineate its neurobehavioral profile in a comprehensive way. Collectively, our results show that MB is a unique mental state supported by a distinct neural state that contributes meaningfully to spontaneous mental activity.

Behaviorally, we found that individuals report MB occurrences less frequently and faster than other mental states. This finding is in line with previous studies showing that MB gets reported significantly less often than thought-related states (6, 10), although the opposite effect was also reported (7). These discrepancies might be attributed to the study protocol, where in the latter study participants were encouraged to stay engaged in thinking about nothing (7). This implies that MB might be a flexible and trainable mental state that, once introduced as an option, can be informative of one's ongoing mental experience. Our results also align with studies reporting similarly short MB reaction times while participants are involved in sustained attention to response tasks (21, 22). Other investigations, though, show that MB can be reported more slowly compared to other mental states, which was interpreted as MB facilitating sluggishness in responses (9) or as the result of decreases in alertness and arousal during task performance (23). Here, we consider that the short reaction times for MB and the longer reaction times for thought-related mental states (Sdep, Sind) might be attributed to an additional cognitive evaluation of the latter. In other words, when thoughts are occupied by specific content, this is translated into longer cognitive evaluation as to the particularities of this content.

This stance implies that MB can be a mental state that is "content-free," and as such it is reported faster. This interpretation is supported by previous investigations using self-paced focused reading with self-catches of MB and mind wandering (6). Although this is a tempting consideration, we recognize that the content-free nature of MB reports could not be directly addressed here. Attempting to uncover the mechanisms of MB, past work shows that attention can act as a mediating process that drives content reportability (24), so that participants do entertain content-full thoughts but fail to attend to them, therefore leading to attentional lapses (22, 23, 25). At the same time, it can be that MB is a matter of participants' metacognitive capacities, in that MB is more about a "cognitive-evaluation free" or "meta-awareness free" mental state rather than lack of mental content. Equally, MB might be deprived of any experience altogether, reflecting a "transition mode" between modifications of experience (content) as we move from one state to the other. This last scenario fits with our results of the low probabilities to report MB when previously in another mental state. In that case, departures from MB are more likely to lead toward thought-related reports and less likely to return to MB. However, these findings should be considered within the temporal constraints of the experience-sampling paradigm, namely, one cannot assume that this dynamic sequencing reflects actual mental state transitions because the temporal structure between the reports is not continuous. Consequently, other mental states might have appeared between reports. Despite this limitation, the finding that the equally small probabilities to report MB when previously in another state and vice versa indicates that MB might not be driven by any specific mental content, therefore serving as a transient mental relay (26). This means that thoughts with reportable content can lead toward more mental contents due to semantic associations, hence creating the perception of a stream of consciousness (2). Since MB is not semantically associated with any particular mental content, it may therefore occur scarcely during ongoing experience. Therefore, phenomenologically "empty" mental states might have less of an anchoring effect than content-full states. Finally, our finding of a uniform distribution of MB reports over time, also reported elsewhere (6, 27), further suggests that MB happens spontaneously across time and is not an artifact of fatigue or sleepiness, which would lead to more occurrences at the end of the recordings. Additionally, in the absence of direct physiological measures of arousal, such as electroencephalography or pupillometry markers, the BOLD GS amplitude can be considered as a proxy of arousal and also sleepiness (28, 29). Although other studies relate sleepiness to an inflated number of MB reports and reduced reaction times (21, 22), the lack of significant correlation between GS amplitude and reaction times shows that sleepiness is not a confounding factor of MB reportability in our dataset. Taken together, the behavioral results indicate that MB is a distinct mental state with a unique position among thought-related reports. In order to shed light on the refined mechanisms underlying MB reportability we suggest that future work address MB in terms of content, attention, and metacognitive capacities.

In terms of MB's neural underpinnings, we first found that the amplitude of the GS was preferentially higher for scanning volumes associated to the MB reports. In addition, the supplementary analysis of the neurobehavioral coupling without the GS confirmed that the GS contributes meaningfully to the MB state as it dramatically changes the overall interregional positive coherence of pattern 3 after its removal. At the moment, we can only speculate about what the high GS amplitude might mean for MB reportability. In terms of physiological relevance, spontaneous GS amplitude was previously found to correlate negatively with electroencephalographic (EEG) vigilance (alpha, beta oscillations), while increases in EEG vigilance due to caffeine ingestion were associated with reduced GS amplitude (30). In macaques, electrocorticography showed that widespread transient and synchronous cortical activity was linked to low arousal in a series of sequential spectral transitions (i.e., from decreases in midfrequency activity, accompanied by increases in the gamma band, to be followed by increases in delta band) (31). When these transient electrophysiological events in animals were linked to fMRI motifs in humans, there was a close association between the GS and these transitions, which corroborated the origins of arousal (32). These results, jointly with the elevated GS amplitude during MB described herein, show the possibility of neuronal silencing during wakefulness.

The scenario of neuronal silencing is further supported by the analysis of neurobehavioral coupling. With this analysis we first showed four distinct brain functional connectivity patterns, which recur dynamically during the resting periods of the experience-sampling task. These brain patterns bear great resemblance to what we previously reported as recurrent brain configurations during pure resting state fMRI acquisitions across healthy individuals and brain-injured patients (16). The fact that these patterns appear across independent datasets, and also in nonhuman primates (33), under different paradigms, different brain parcellations, and different cluster sizes, points to their universality and robustness. Specifically to MB, the pattern with the all-to-all positive interareal connectivity (pattern 3) had the highest

similarity to the connectivity matrices preceding MB reports. Such high prevalence of comparable signal configurations was previously shown during non–rapid eye movement slow-wave sleep, wherein overall minimal neuronal firing was translated as globally positive connectivity (34, 35). Studies in rats (36) show that such periods of neuronal silencing can happen also during wakefulness in the form of neuronal firing rate reduction, leading to slow wave activity, which is indicative of local sleeps. When applied to humans, it has been argued that these instances of local sleeps can be the phenomenological counterpart of MB (9). In that respect, wakefulness does not only support constantly on periods of neuronal function. Rather, our brains can also show instances of neural down states even during wakefulness, possibly for homeostatic reasons (37), which can be translated as global positive connectivity and phenomenologically interpreted as MB.

From theoretical perspective, it seems that MB further challenges the boundaries of various models of conscious experience. For example, the global neuronal workspace theory (38) posits that a stimulus becomes reportable when some of its locally processed information becomes available to a wide range of brain regions, forming a balanced distributed network (39). A key process of this global broadcasting is ignition (40). Ignition is characterized by the sudden, coherent, and exclusive activation of a subset of workspace neurons that code a particular content, while the remainder of the workspace neurons stay inhibited. If the global neuronal workspace ignition is always related to selective neural activation and inhibition (content), the theory cannot account for how MB can still be reported if it is linked to a functional connectome with only positive connections. This is similar for the integrated information theory (IIT) (41). According to it, in order to generate an experience, a physical system must be able to discriminate between a large repertoire of states (i.e., information). This must be done as a single system that cannot be decomposed into a collection of causally independent parts (i.e., integration). So far, the IIT can explain the inability to report mental content in brain states with extreme functional integration (i.e., functional hyperconnectivity), as during generalized epilepsy (42). In such a brain state, an abnormally large number of regions work in synchrony, and, as a result, the brain becomes no longer capable of processing information in a way that leads to conscious experience. The here-identified all-to-all positive connectivity pattern shows the highest level of integration and efficiency and the lowest level of segregation and modularity compared to the other brain patterns (16). Therefore, this may imply that such a neural configuration is unable to produce a balance between values of integrated information and segregation of it, leading to limited experience, such as MB. If the role of integration is emphasized over the role of segregation, as in the recent version of IIT, then MB challenges that approach, making a clear case for the importance of segregation of information within neural configurations of conscious content. Importantly, though, the integration in IIT happens only when there is a content of experience, being reported or not, which is totally counterintuitive for MB. Both theories essentially start from the premise that experience is made up of various bits from which a unified experience arises. As MB does not provide such building blocks, it seems to be a kind of global state of unified experience, with conscious content being the modifications of such a basal conscious field, according to Searle's unified field model (43). If this interpretation is considered, then the current findings pose an important challenge to building block models of conscious experience.

Our analysis leaves several questions unaddressed. First, the current design does not permit us to determine the underlying mechanism that drives MB (i.e., whether it is an effect of attention, memory, or language). Such determination is expected to shed light on MB's modulatory mechanisms as well and therefore further indicate its functional significance in variant conditions. Second, apart from the intrinsic problems with the validity and reliability of self-reports during experience sampling (44), we also used a probe-catching method. This means that participants were interrupted during spontaneous thinking by a probe, asking them to choose an appropriate option to describe their thought state. Such a probe-framing technique can restrict the estimation of potential phenomenological switches happening in between. Indeed, as the probes were appearing at predetermined time points, we cannot exclude the possibility of mental contents happening during the interprobe intervals, and hence they were missed to be reported. Also, probe framing can be suboptimal in capturing spontaneous thinking because it might lead to an inflated number of MB reports. This is because participants may have chosen this category becasue it was available, which, otherwise, they would not have reported if they were to identify it spontaneously (45). However, given that MB occurrences were not reported with a comparable high frequency to the content-oriented states, it might be that MB was evaluated in a representative way across the evaluation, leading to infrequent occurrences across participants. Third, the high repetition time (TR) during the fMRI acquisition (2.04 s) could also have echoed the temporal implications of the MB profiling. By means of simultaneous EEG and fMRI recordings, more light is expected to be shed on fine-grained temporal dynamics of MB. Such simultaneous multimodal recordings are expected to also illuminate the assumption of slow-wave activity as the corresponding neural mechanism of MB. Finally, we cannot exclude the possibility that the mind is not absent in the first place, under the premise that if it were, participants would not have been able to report anything, including its absence. The term "mind blanking", thus, may reflect different aspects (e.g., truly absence of the mind vs. absence of conscious access to mental events) that still need to be disentangled.

In conclusion, our study suggests that MB can be considered a default mental state occupying a unique position among thought-related reports. Its rigid neurofunctional profile could account for the inability to report mental content due to the brain's inability to differentiate signals in an informative way. While we wait for the underlying mechanisms of MB to be illuminated, these data suggest that instantaneous nonreportable mental events can happen during wakefulness, setting MB as a prominent mental state during ongoing experience.

Materials and Methods

Dataset. Thirty-six healthy right-handed adults participated in an fMRI experience-sampling task (3). This sample size has been shown sufficiently reliable for group-level fMRI (46). All participants gave their written informed consent to take part in the experiment. The ethics committee of the University Hospital of Liège approved the study. Data were acquired during resting state while participants were lying inside the scanner with eyes open. At random times, they were interrupted by an auditory tone, probing them to report their immediate mental state via button presses (Fig. 1, *Upper panel*). The sampling probes were randomly distributed between 30 and 60 s. Each probe started with the appearance of an exclamation mark lasting for 1,000 ms, inviting the participants to review and characterize the cognitive events they just experienced. Then, on the screen four categories for a broad characterization of the cognitive experiences were shown: absence, perception, stimulus-dependent thought, and stimulus-independent thought. Absence was defined as mind blanking or empty state of mind. Perceptions represented the acknowledgment of a stimulus through one or more senses without any internal

thought. Thoughts were distinguished as stimulus-dependent (i.e., with awareness of the immediate environment), or stimulus-independent (i.e., with no awareness of the immediate environment). For reporting, participants used two response boxes, one in each hand. Participants used an egocentric mental projection of their fingers onto the screen so that each finger corresponded to a specific mental category. Depending on the probes' trigger times and participants' reaction times, the duration of the recording session was variable (48–58 min). To minimize misclassification rates, participants had a training session outside the scanner at least 24 h before the actual session.

Imaging Setup. Experiments were carried out on a 3-T head-only scanner (Magnetom Allegra, Siemens Medical Solutions, Erlangen, Germany) operated with the standard transmit–receive quadrature head coil. fMRI data were acquired via a T2*-weighted gradient-echo echo-planar imaging sequence with the following parameters: TR = 2,040 ms, echo time = 30 ms, field of view = 192 × 192 mm^2, 64 × 64 matrix, 34 axial slices with 3 mm thickness and 25% interslice gap to cover most of the brain. A high-resolution T1-weighted magnetization-prepared rapid gradient echo image was acquired for anatomical reference (TR = 1,960 ms, echo time = 4.4 ms, inversion time = 1,100 ms, field of view = 230 × 173 mm, matrix size = 256 × 192 × 176, voxel size = 0.9 × 0.9 × 0.9 mm). The participant's head was restrained with a vacuum cushion to minimize head movement. Stimuli were displayed on a screen positioned at the rear of the scanner, which the participant could comfortably see via a head coil–mounted mirror.

Behavioral Analysis. Analyses were performed with locally developed codes in Python and R. Six paired *t* tests were used to compare the number of reports of each mental state across participants (*P* values were FDR corrected with a significance level of $\alpha = 0.05$). A generalized linear mixed model with a gamma distribution and inverse link function (47) tested the relationship between reaction times and mental states. The choice of the generalized linear mixed model was because of positive tail in the distribution of reaction times and inhomogeneity of variance across mental states caused by an imbalanced number of reports. Mental state reports were considered as fixed effects, and participants were considered as the random effects, with sex and age as confound variables. In case of significant main effects, a post hoc test was applied for pairwise comparisons. For that, we used the Tukey method to correct the type I error inflation that occurred in the multiple comparisons. To model dynamic transition between mental state reports, a Markov model was used to calculate the transition probabilities between participants' reports over the experiment. The uniformity of the distribution of each report over the acquisition duration was tested via χ^2 test on the time point of reports across all participants. The acquisition duration of each subject was divided into 10 equal temporal bins, and the number of reports in each bin was counted. To calculate the effect size of the χ^2 test, φ measure was used ($\varphi = \sqrt{\frac{\chi^2}{n}}$, where *n* is the number of observations).

fMRI Preprocessing. Preprocessing and denoising were performed via a locally developed pipeline written in Python [nipype package (48)] encompassing toolboxes from Statistical Parametric Mapping 12 (49), FSL 6.0 (50), AFNI (51), and ART (http://web.mit.edu/swg/software.htm). In this pipeline, all the functional volumes were realigned to the first volume and then, in a second pass, to their average. Estimated motion parameters were then used for artifact detection. An image was defined as an outlier or artifact image if the head displacement in the *x*, *y*, or *z* direction was greater than 3 mm from the previous frame, if the rotational displacement was greater than 0.05 rad from the previous frame, or if the global mean intensity in the image was more than 3 SD from the mean image intensity for the entire scans. After skull-stripping of structural data [using FSL BET (52) with fractional intensity of 0.3], realigned functional images were registered to the bias-corrected structural image in the subject space (rigid body transformation with normalized mutual information cost function). After white matter (WM), gray matter (GM), and cerebrospinal fluid (CSF) masks were extracted, all the data and masks were transformed into the standard stereotaxic Montreal Neurological Institute space (MNI152 with 2-mm resolution). WM and CSF masks were further eroded by one voxel. For noise reduction, we modeled the influence of noise as a voxel-specific linear combination of multiple empirically estimated noise sources by deriving the first five principal components from WM and CSF masked functional data separately. These nuisance regressors together with detected outlier volumes, motion parameters, and their first-order derivative were used to create a design matrix in the first-level general linear model (GLM). After the functional data were smoothed with a Gaussian kernel of 6 mm full width at half-maximum, the designed GLM was fitted to the data. Before GLM was applied, functional data were demeaned and detrended and all the motion-related and tissue-based regressors were first normalized and then demeaned and detrended via the approach explained in (53). A temporal causal bandpass filter of 0.01–0.04 Hz was then applied on the residuals of the model to extract low-frequency fluctuations of the BOLD signal. Schaefer atlases (54) with 100 ROIs were then used to parcellate each individual brain. The average of voxel time series in each region was considered as the extracted ROI time series and was used for further analysis.

All eventual connectivity analyses were performed with both the inclusion and the removal of GS. This is because in resting state analyses a great debate concerns the removal or not of the GS (14). To date, there is support for both views. The GS has been shown to have a neuronal counterpart (15, 20) that promotes behavior (13). It was also shown to reflect fMRI nuisance sources such as motion, scanner artifacts, respiration (55), cardiac rate (56), and vascular activity (57, 58).

Functional Connectivity Pattern Estimation. We used the phase-based coherence analysis to extract between-region connectivity patterns at each time point of the scanning session (16). For each participant *i*, after *z*-normalization of time series at each region *r* (i.e., $x_{i,r}[t]$), the instantaneous phase of each time series was calculated via Hilbert transform as:

$$\hat{x}_{i,r}(t) = \frac{1}{\pi t} * x_{i,r}(t), \quad [1]$$

where * indicates a convolution operator. Using this transformation, we produced an analytical signal for each regional time series as:

$$X^a_{i,r}(t) = x_{i,r}(t) + j\hat{x}_{i,r}(t), \quad [2]$$

where $j = \sqrt{-1}$. From this analytical signal, the instantaneous phase of each time series can be estimated as:

$$\varphi_{i,r}(t) = \tan^{-1}\left(\frac{\hat{x}_{i,r}(t)}{x_{i,r}(t)}\right). \quad [3]$$

After wrapping each instantaneous phase signal of $\varphi_{i,r}(t)$ to the $[-\pi,\pi]$ interval and naming the obtained signal as $\theta_{i,r}(t)$, we calculated a connectivity measure for each pair of regions as the cosine of their phase difference. For example, the connectivity measure between regions *r* and *s* in subject *i* was defined as:

$$conn_{i,r,s}(t) \triangleq \cos(\theta_{i,r}(t) - \theta_{i,s}(t)). \quad [4]$$

By this definition, completely synchronized time series lead to a connectivity value of 1, completely desynchronized time series produce a connectivity value of zero, and anticorrelated time series produce a connectivity measure of −1. Using this approach, we created a connectivity matrix of 100 × 100 at each time point *t* for each subject *i* that we called $C_i(t)$:

$$C_i(t) \triangleq [conn_{i,r,s}(t)]_{r,s}. \quad [5]$$

After collecting connectivity matrices of all time points of all participants, we applied *k*-means clustering on all estimated connectivity matrices. With this technique, four robust and reproducible patterns were extracted as the centroids of the clusters, and each resting connectivity matrix was assigned to one of the extracted patterns. [We chose to extract four patterns to compare our results with our previous research (16). However, we replicated all the analyses using different numbers of clusters ranging from 3 to 7.] We calculated the occurrence rate of each pattern simply by counting the number of matrices that were assigned to each specific pattern at each subject separately. Significant differences between pattern occurrence rates were analyzed via paired *t* test and FDR correction of *P* values over six possible pairwise comparisons.

Classification of MB Based on Time-Varying Connectivity Matrices. Phase-based coherence matrices within the analysis windows were considered as the feature vectors and the related mental state reports as the class labels. First, an SVM model for binary classification was designed to classify MB reports from all the other reports. As the dataset was imbalanced, we calculated precision ($\frac{TP}{TP+FP}$), recall ($\frac{TP}{TP+FN}$), and balanced accuracy ($\frac{1}{2}(\frac{TP}{TP+FN} + \frac{TN}{TN+FP})$) as the efficiency parameters of the classifier (TP, true positive; TN, true negative; FP, false positive;

FN, false negative; MB reports were defined as positive class). To compute balanced accuracy, each sample was weighted according to the inverse prevalence of its true class, which accordingly avoids inflated performance estimates on imbalanced datasets. Recall (a parameter between 0 and 1) is the ability of the classifier to classify positive samples correctly. Because the number of MB reports is much less than that of the other mental states, a high recall score shows that the classifier is not biased toward the larger classes. Precision (a parameter between 0 and 1) is also defined as the ability of the classifier not to label as positive a sample that is negative (https://scikit-learn.org/stable/modules/model_evaluation.html). A high precision also shows that classifier is not biased toward larger classes. As the cross-validation strategy, a fivefold stratified cross-validation with 10 repeats was applied. This classification strategy was also repeated for a one-versus-one classification of MB versus each of the other reports separately. To compare the results with an empirical chance level, a dummy classifier was also used to classify MB from other reports. This dummy classifier generated random predictions by respecting the training set class distribution.

Neurobehavioral Coupling. To evaluate the similarity between mental states' functional connectivity patterns and the main resting state recurrent functional configurations, we extracted the five connectivity matrices preceding each probe as the functional repertoire of each specific mental state and then calculated their cosine similarity to the main resting state patterns. In order to consider the effect of hemodynamic response, all analyses were performed on the shifted versions of the connectivity matrices with time lags ranging from zero (five matrices before the probe) to three (two preprobe and three postprobe matrices). The selection of this time window was justified by the fact that ongoing experience can fluctuate slowly with a period of ∼10 s (3), as well as by the nature of the hemodynamic response that reaches its maximum after three postevent scans (59). Other values can also be considered as the analysis window length; for example, in (60) a 6-s analysis window was suggested. This can be important due to the temporal dynamics of the ongoing experience. In fact, long analysis windows can lead to blurring together of multiple mental states, while short analysis windows can reduce the signal-to-noise ratio in the subsequent analyses. Cosine similarity between two sample matrices of A and B can be calculated as:

$$dist(A,B) = \frac{Tr(A^T B)}{\sqrt{Tr(A^T A)Tr(B^T B)}}, \quad [6]$$

where Tr(.) indicates trace of a matrix. Cosine similarity determines how similar two matrices/vectors are irrespective of their norm. It can be considered as the normalized version of the Euclidean distance (i.e., projecting the vectors onto the unit sphere and calculating Euclidean distance, which is then effectively the cosine of the angle between those vectors). Subsequently, for each mental state the distribution of distances to all four centroids was created. A generalized linear mixed effect model with gamma distribution and log link function was applied to test the relationship between the distances to each pattern and the mental states. In this model, all mental state reports were considered as fixed effects and participants as random effects, with sex and age as confound variables. To correct for the multiple comparison problem due to fitting the model to the distance values of different patterns separately, an effect was considered significant if its P value was less than $0.05/K$, where K is the number of patterns. In the case of a significant effect, a Tukey post hoc test was applied to compare each pair of mental states separately and to correct the type I error inflation due to multiple comparisons.

GS Effect Analysis. We calculated the GS for each subject after applying the atlas and time series extraction, by averaging time series of all the ROIs. To study the effect of the GS on the analysis results, we subtracted it once from the time series related to each ROI (GSS):

$$x'_{i,r}(t) = x_{i,r}(t) - g_i(t), \quad [7]$$

where i identifies the subject, r identifies the ROI, and $g_i(t)$ is the GS of the subject i, and regressed it out once from the ROI time series (GSR):

$$x'_{i,r}(t) = x_{i,r}(t) - \frac{|x_{i,r}(t)|}{|g_i(t)|}.corr(x_{i,r}(t), g_i(t))g_i(t). \quad [8]$$

All analyses related to the connectivity pattern extraction, their occurrence rate, and neurobehavioral coupling were also repeated in these signal versions. To study the relationship between GS and mental states, the GS amplitude was calculated for each mental state. The GS amplitude was defined as the sum of the absolute value of the five GS time points related to the functional repertoire of each mental state. A generalized mixed effect model with gamma distribution and inverse link function was fitted to the GS amplitude values, considering mental states as main effect and subjects as random effect of the model. In case of finding a significant effect, a Tukey post hoc test was performed to compare each pair of the mental states in terms of their related GS amplitude.

Data, Materials, and Software Availability. Preprocessed functional data at the level of ROI time series can be freely downloaded from: https://osf.io/3vqb6/download. The raw data are also freely available in BIDS format from: https://openneuro.org/datasets/ds004134/versions/1.0.0.

All the preprocessing and analysis codes are freely available on GitLab: https://gitlab.uliege.be/S.Mortaheb/mind_blanking.

Anonymized data (raw data; preprocessed functional data; preprocessing and analysis codes) have been deposited in OpenNeuro, OSF, and GitLab (10.18112/openneuro.ds004134.v1.0.0; https://osf.io/3vqb6/download; https://gitlab.uliege.be/S.Mortaheb/mind_blanking) (61, 62).

ACKNOWLEDGMENTS. This work was supported by the Belgian Fund for Scientific Research (FNRS). S. Mortaheb is a research fellow, A. Demertzi is a research associate, and S. Majerus is a research director at the FNRS. We also thank Dr. Matthieu Koroma, Dr. Camilo Miguel Signorelli, and Mr. Larry D. Fort for proofreading and editing the manuscript. This article is based upon work from COST Action CA18106, supported by COST (European Cooperation in Science and Technology).

Author affiliations: [a]Cyclotron Research Center In Vivo Imaging, GIGA Institute, University of Liège, Liège, Belgium; [b]Fund for Scientific Research (FNRS), Brussels, Belgium; [c]Institute of Neuroscience and Medicine, Brain and Behaviour (INM-7), Research Centre Jülich, Jülich, Germany; [d]Institute of Systems Neuroscience, Medical Faculty, Heinrich Heine University Düsseldorf, Düsseldorf, Germany; [e]Department of Psychology, CITY College, University of York Europe Campus, Thessaloniki, Greece; [f]Psychology and Neuroscience of Cognition Research Unit, University of Liège, Liège, Belgium; [g]Institute of Bioengineering, École Polytechnique Fédérale de Lausanne, Switzerland; and [h]Department of Radiology and Medical Informatics, University of Geneva, Geneva, Switzerland

1. J. Smallwood *et al.*, The neural correlates of ongoing conscious thought. *iScience* **24**, 102132 (2021).
2. K. Christoff, Z. C. Irving, K. C. R. Fox, R. N. Spreng, J. R. Andrews-Hanna, Mind-wandering as spontaneous thought: A dynamic framework. *Nat. Rev. Neurosci.* **17**, 718–731 (2016).
3. L. Van Calster, A. D'Argembeau, E. Salmon, F. Peters, S. Majerus, Fluctuations of attentional networks and default mode network during the resting state reflect variations in cognitive states: Evidence from a novel resting-state experience sampling method. *J. Cogn. Neurosci.* **29**, 95–113 (2017).
4. T. Karapanagiotidis, B. C. Bernhardt, E. Jefferies, J. Smallwood, Tracking thoughts: Exploring the neural architecture of mental time travel during mind-wandering. *Neuroimage* **147**, 272–281 (2017).
5. A. Turnbull *et al.*, Left dorsolateral prefrontal cortex supports context-dependent prioritisation of off-task thought. *Nat. Commun.* **10**, 3816 (2019).
6. A. F. Ward, D. M. Wegner, Mind-blanking: When the mind goes away. *Front. Psychol.* **4**, 650 (2013).
7. T. Kawagoe, K. Onoda, S. Yamaguchi, The neural correlates of "mind blanking": When the mind goes away. *Hum. Brain Mapp.* **40**, 4934–4940 (2019).
8. T. Andrillon *et al.*, Does the mind wander when the brain takes a break? Local sleep in wakefulness, attentional lapses and mind-wandering. *Front. Neurosci.* **13**, 949 (2019).
9. T. Andrillon, A. Burns, T. Mackay, J. Windt, N. Tsuchiya, Predicting lapses of attention with sleep-like slow waves. *Nat. Commun.* **12**, 3657 (2021).
10. J. W. Schooler, E. D. Reichle, D. V. Halpern, "Zoning out while reading" in *Thinking and Seeing: Visual Metacognition in Adults and Children*, D. T. Levin, Ed. (MIT Press, 2004), pp. 203–226.
11. T. Kawagoe, K. Onoda, S. Yamaguchi, Different pre-scanning instructions induce distinct psychological and resting brain states during functional magnetic resonance imaging. *Eur. J. Neurosci.* **47**, 77–82 (2018).
12. U. Winter *et al.*, Content-free awareness: EEG-fcMRI correlates of consciousness *as Such* in an expert meditator. *Front. Psychol.* **10**, 3064 (2020).
13. J. Li *et al.*, Global signal regression strengthens association between resting-state functional connectivity and behavior. *Neuroimage* **196**, 126–141 (2019).

14. K. Murphy, M. D. Fox, Towards a consensus regarding global signal regression for resting state functional connectivity MRI. *Neuroimage* **154**, 169–173 (2017).
15. M. L. Schölvinck, A. Maier, F. Q. Ye, J. H. Duyn, D. A. Leopold, Neural basis of global resting-state fMRI activity. *Proc. Natl. Acad. Sci. U.S.A.* **107**, 10238–10243 (2010).
16. A. Demertzi, *et al.*, Human consciousness is supported by dynamic complex patterns of brain signal coordination. *Sci. Adv.* **5**, eaat7603 (2019).
17. N. Leonardi *et al.*, Principal components of functional connectivity: A new approach to study dynamic brain connectivity during rest. *Neuroimage* **83**, 937–950 (2013).
18. J. S. Anderson *et al.*, Network anticorrelations, global regression, and phase-shifted soft tissue correction. *Hum. Brain Mapp.* **32**, 919–934 (2011).
19. K. Murphy, R. M. Birn, D. A. Handwerker, T. B. Jones, P. A. Bandettini, The impact of global signal regression on resting state correlations: Are anti-correlated networks introduced? *Neuroimage* **44**, 893–905 (2009).
20. H. Xu *et al.*, Impact of global signal regression on characterizing dynamic functional connectivity and brain states. *Neuroimage* **173**, 127–145 (2018).
21. D. Stawarczyk, A. D'Argembeau, Conjoint influence of mind-wandering and sleepiness on task performance. *J. Exp. Psychol. Hum. Percept. Perform.* **42**, 1587–1600 (2016).
22. D. Stawarczyk, C. François, J. Wertz, A. D'Argembeau, Drowsiness or mind-wandering? Fluctuations in ocular parameters during attentional lapses. *Biol. Psychol.* **156**, 107950 (2020).
23. N. Unsworth, M. K. Robison, Pupillary correlates of lapses of sustained attention. *Cogn. Affect. Behav. Neurosci.* **16**, 601–615 (2016).
24. M. A. Pitts, L. A. Lutsyshyna, S. A. Hillyard, The relationship between attention and consciousness: An expanded taxonomy and implications for 'no-report' paradigms. *Philos. Trans. R. Soc. Lond. B Biol. Sci.* **373**, 20170348 (2018).
25. C. Van den Driessche *et al.*, Attentional lapses in attention-deficit/hyperactivity disorder: Blank rather than wandering thoughts. *Psychol. Sci.* **28**, 1375–1386 (2017).
26. A. Fornito, B. J. Harrison, A. Zalesky, J. S. Simons, Competitive and cooperative dynamics of large-scale brain functional networks supporting recollection. *Proc. Natl. Acad. Sci. U.S.A.* **109**, 12788–12793 (2012).
27. F. N. Watts, A. K. MacLeod, L. Morris, Associations between phenomenal and objective aspects of concentration problems in depressed patients. *Br. J. Psychol.* **79**, 241–250 (1988).
28. M. Fukunaga *et al.*, Large-amplitude, spatially correlated fluctuations in BOLD fMRI signals during extended rest and early sleep stages. *Magn. Reson. Imaging* **24**, 979–992 (2006).
29. G. Nilsonne *et al.*, Intrinsic brain connectivity after partial sleep deprivation in young and older adults: Results from the Stockholm Sleepy Brain study. *Sci. Rep.* **7**, 9422 (2017).
30. C. W. Wong, V. Olafsson, O. Tal, T. T. Liu, The amplitude of the resting-state fMRI global signal is related to EEG vigilance measures. *Neuroimage* **83**, 983–990 (2013).
31. X. Liu *et al.*, Arousal transitions in sleep, wakefulness, and anesthesia are characterized by an orderly sequence of cortical events. *Neuroimage* **116**, 222–231 (2015).
32. X. Liu *et al.*, Subcortical evidence for a contribution of arousal to fMRI studies of brain activity. *Nat. Commun.* **9**, 395 (2018).
33. P. Barttfeld *et al.*, Signature of consciousness in the dynamics of resting-state brain activity. *Proc. Natl. Acad. Sci. U.S.A.* **112**, 887–892 (2015).
34. F. Aedo-Jury, M. Schwalm, L. Hamzehpour, A. Stroh, Brain states govern the spatio-temporal dynamics of resting-state functional connectivity. *eLife* **9**, 1–23 (2020).
35. M. El-Baba *et al.*, Functional connectivity dynamics slow with descent from wakefulness to sleep. *PLoS One* **14**, e0224669 (2019).
36. V. V. Vyazovskiy *et al.*, Local sleep in awake rats. *Nature* **472**, 443–447 (2011).
37. M. C. D. Bridi *et al.*, Daily oscillation of the excitation–inhibition balance in visual cortical circuits. *Neuron* **105**, 621–629.e4 (2020).
38. S. Dehaene, J. P. Changeux, L. Naccache, J. Sackur, C. Sergent, Conscious, preconscious, and subliminal processing: A testable taxonomy. *Trends Cogn. Sci.* **10**, 204–211 (2006).
39. C. Sergent, S. Dehaene, Neural processes underlying conscious perception: Experimental findings and a global neuronal workspace framework. *J. Physiol. Paris* **98**, 374–384 (2004).
40. S. Dehaene, C. Sergent, J. P. Changeux, A neuronal network model linking subjective reports and objective physiological data during conscious perception. *Proc. Natl. Acad. Sci. U.S.A.* **100**, 8520–8525 (2003).
41. G. Tononi, Consciousness as integrated information: A provisional manifesto. *Biol. Bull.* **215**, 216–242 (2008).
42. H. Blumenfeld, Impaired consciousness in epilepsy. *Lancet Neurol.* **11**, 814–826 (2012).
43. J. R. Searle, Consciousness. *Annu. Rev. Neurosci.* **23**, 557–578 (2000).
44. R. E. Nisbett, T. D. Wilson, Telling more than we can know: Verbal reports on mental processes. *Psychol. Rev.* **84**, 231–259 (1977).
45. Y. Weinstein, H. J. De Lima, T. van der Zee, Are you mind-wandering, or is your mind on task? The effect of probe framing on mind-wandering reports. *Psychon. Bull. Rev.* **25**, 754–760 (2018).
46. B. Thirion *et al.*, Analysis of a large fMRI cohort: Statistical and methodological issues for group analyses. *Neuroimage* **35**, 105–120 (2007).
47. C. J. Anderson, J. Verkuilen, T. R. Johnson, *Applied Generalized Linear Mixed Models : Continuous and Discrete Data* (Springer, 2010).
48. K. Gorgolewski *et al.*, Nipype: A flexible, lightweight and extensible neuroimaging data processing framework in python. *Front. Neuroinform.* **5**, 13 (2011).
49. W. D. Penny, K. J. Friston, J. T. Ashburner, S. J. Kiebel, T. E. Nichols, *Statistical Parametric Mapping: The Analysis of Functional Brain Images* (Elsevier, 2011).
50. M. Jenkinson, C. F. Beckmann, T. E. J. Behrens, M. W. Woolrich, S. M. Smith, FSL. *Neuroimage* **62**, 782–790 (2012).
51. R. W. Cox, AFNI: Software for analysis and visualization of functional magnetic resonance neuroimages. *Comput. Biomed. Res.* **29**, 162–173 (1996).
52. S. M. Smith, Fast robust automated brain extraction. *Hum. Brain Mapp.* **17**, 143–155 (2002).
53. J. D. Power *et al.*, Methods to detect, characterize, and remove motion artifact in resting state fMRI. *Neuroimage* **84**, 320–341 (2014).
54. A. Schaefer *et al.*, Local-global parcellation of the human cerebral cortex from intrinsic functional connectivity MRI. *Cereb. Cortex* **28**, 3095–3114 (2018).
55. J. D. Power, M. Plitt, T. O. Laumann, A. Martin, Sources and implications of whole-brain fMRI signals in humans. *Neuroimage* **146**, 609–625 (2017).
56. C. Chang, G. H. Glover, Time-frequency dynamics of resting-state brain connectivity measured with fMRI. *Neuroimage* **50**, 81–98 (2010).
57. D. C. Zhu, T. Tarumi, M. A. Khan, R. Zhang, Vascular coupling in resting-state fMRI: Evidence from multiple modalities. *J. Cereb. Blood Flow Metab.* **35**, 1910–1920 (2015).
58. N. Colenbier *et al.*, Disambiguating the role of blood flow and global signal with partial information decomposition. *Neuroimage* **213**, 116699 (2020).
59. H. J. Aizenstein *et al.*, The BOLD hemodynamic response in healthy aging. *J. Cogn. Neurosci.* **16**, 786–793 (2004).
60. M. Sormaz *et al.*, Default mode network can support the level of detail in experience during active task states. *Proc. Natl. Acad. Sci. U.S.A.* **115**, 9318–9323 (2018).
61. S. Mortaheb *et al.*, Experience Sampling in Resting State. OpenNeuro. https://openneuro.org/datasets/ds004134/versions/1.0.0. Deposited 27 May 2022.
62. S. Mortaheb, Mind_Blanking. gitlab. https://gitlab.uliege.be/S.Mortaheb/mind_blanking. Accessed 20 September 2022.